Analysis of Fracture Data of Conductive Cracks in Lead Zirconate Titanate PIC 151 Ceramics with the Charge-free Zone Model

Tong-Yi Zhang
Mechanical Engineering Department, The Hong Kong University of Science and Technology, Clear Water Bay, Kowloon, Hong Kong, China

Abstract: The charge-free zone model for electrically conductive cracks in piezoelectric ceramics is reviewed and applied to interpret the experimental results on poled lead zirconate titanate PIC 151 ceramics. Good agreement between the experimental results and the charge-free zone model indicates again that the concepts of fracture mechanics can be applied to the failure of conductive cracks in piezoelectric ceramics.

Keywords: Piezoelectric ceramics, Fracture, Conductive cracks, Charge-free zone model, Mechanical and/or electric loading

1. Introduction

Piezoelectric ceramics have become preferred materials for a wide variety of electronic and mechatronic devices and structures due to their pronounced dielectric, piezoelectric, and pyroelectric properties. However, aging, fatigue and electrical and/or mechanical breakdown may occur in and lead to failure of the materials. Furthermore, piezoelectric ceramics are brittle and susceptible to cracking at all scales from electric domains to electronic devices. Due to the importance of electrical and mechanical reliability of devices and structures made of piezoelectric ceramics, there has been tremendous interest in studying the fracture behavior of such materials [1-6]. Yang [7], Zhang *et al.* [8] and Chen and Lu [9] provided overviews on fracture of piezoelectric ceramics. These overviews summarized the current knowledge on the fracture of piezoelectric ceramics including the theoretical development of piezoelectric fracture mechanics and the experimental achievement on the failure behavior of piezoelectric ceramics under mechanical and/or electrical loading. In the overview article [9], Chen and Lu gave a detailed discussion about the strip polarization saturation model [4] as the premier nonlinear model. Later, Zhang and Gao [10] reviewed new developments in the research on fracture of piezoelectric ceramics and introduced two new models, namely, the dielectric breakdown model and the charge-free zone model. Schneider [11] reviewed experimental results that allow one to interpret the essential features of fracture in ferroelectric ceramics under electric and/or mechanical loading.

Internal electrodes have widely been adopted in electronic and electromechanical devices made of piezoelectric ceramics. These embedded electrodes may naturally function as pre-conductive cracks or notches if Young's modulus of the electrode is much smaller than Young's modulus of the ceramics.

In addition, dielectric breakdown and partial discharge may convert an originally electrically insulating crack to an electrically conductive crack. Figure 1 schematically shows the similarity between a conductive crack under electrical loading and a conventional crack under mechanical loading. To ensure that the electric field inside the conductive crack remains zero, electric charges in the conductive crack surfaces rearrange themselves to produce an induced field that has the same magnitude as the applied one but with an opposite sign. As a result, the charges in the upper and lower crack surfaces near the crack tip have the same sign, as shown in Fig. 1. Charges with the same sign repel each other and have a tendency to propagate the crack. Garboczi [12] studied the contour-independent *J*-integral, which is a fundamental concept in fracture mechanics, for conductive cracks in dielectric materials. The *J*-integral for a conductive crack in a dielectric material under purely electric loading is similar to the *J*-integral for a conventional crack under purely mechanical loading, which is shown in Fig. 1 as well. It is therefore of practical importance and academic significance to apply the concepts of fracture mechanics to the failure of conductive cracks in piezoelectric and dielectric ceramics.

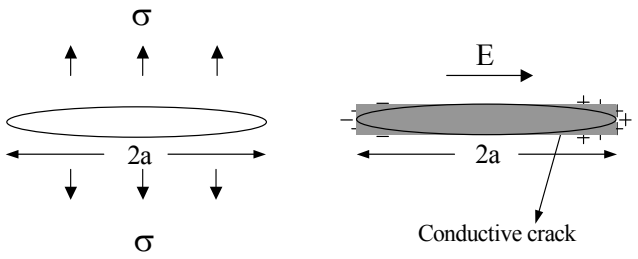

$$J^M = C_M \sigma^2 a \qquad J^E = C_E E^2 a$$

Fig. 1 A comparison of a normal crack subjected to remote uniform mechanical stress, σ, and a conductive crack subjected to remote uniform electrical field, *E*. J^M and J^E denote, respectively, the mechanical and electrical *J*-integrals, and $C_M = \pi / Y^*$ and $C_E = \pi\kappa / 2$, where $Y^* = Y$ for plane stress or $Y^* = Y/(1-\nu^2)$ for plane strain, *Y*, ν and κ are, respectively, the Young's modulus, Poisson ratio, and dielectric constants of the material.

Heyer *et al*. [13] studied the electromechanical fracture toughness of conductive cracks in PZT-PIC ceramics. They conducted four-point bending tests on pre-notched bars, in which the poling direction was toward the jig surface and the notch was filled with NaCl solution to make the crack conducting. Wide-scattering results were obtained under a large applied electric field of $|K_E| > 50 kV/m^{1/2}$, where K_E is the applied electric intensity factor. The critical stress intensity factor increased as the applied electric intensity factor changed from $30 kV/m^{1/2}$ to $-90 kV/m^{1/2}$. When the applied electric intensity factor was relatively small, within the range of $-15 kV/m^{1/2}$ to $15 kV/m^{1/2}$, they could

explain the experimental data using a domain-switching-based model. Using compact tension samples with conductive notches, Wang and Zhang [14] and Fu *et al.* [15] performed extensive fracture tests on thermally depoled and poled lead zirconate titanate (PZT-4) ceramics under purely electrical or mechanical loading. Their experimental results indicate that both the purely electric and mechanical fields can propagate conductive cracks (notches) and fracture the samples. Under purely electric loading, there exists a critical energy release rate at fracture, which is named the electric toughness. The electric toughness is much larger than the mechanical toughness, i.e., the critical energy release rate at fracture under purely mechanical loading. The high electric toughness was attributed to great energy dissipation around the conductive crack tip under purely electric loading, which is impossible under mechanical loading in the brittle electroceramics.

To understand the experimentally observed failure behaviors of conductive cracks in dielectric and piezoelectric ceramics under electric and/or mechanical loading [14, 15], Zhang et al. [16-18] proposed the Charge-Free Zone (CFZ) model by analogy to the dislocation-free zone model. The CFZ model treats dielectric and piezoelectric ceramics as mechanically brittle and electrically ductile. Charge emissions occur at the conductive crack tip and the emitted charges are entrapped in front of the tip. The entrapped charges partially shield the crack tip from the applied electrical field and the local electric intensity factor has a non-zero value. Consequently, there is a non-zero local electric energy release rate, which contributes to the driving force to propagate the conductive crack. The merit of the CFZ model lies in the ability to directly apply the Griffith criterion to link the local energy release rate to the fracture toughness in a purely brittle manner. As a result, the CFZ model provides an explicit failure criterion for predicting the failure behavior of conductive cracks in dielectric and piezoelectric ceramics under electrical and/or mechanical loading. For piezoelectric ceramics [17, 18], the failure formula has an elliptic shape in terms of the normalized electric intensity factor and the normalized stress intensity factor. When the normalized stress intensity factor is set as the horizontal axis, the major semi-axis of an elliptic shape is rotated anticlockwise 45º or -45º if the applied electric field is parallel or anti-parallel to the poling direction. For dielectric ceramics with zero piezoelectric constants, the failure formula is reduced to a quarter of unit circle [16]. The advantage of applying such a failure criterion lies in the ability to predict the critical electric field and the critical mechanical load at which a dielectric or piezoelectric ceramic material containing a conductive crack or an internal electrode fails under electrical and/or mechanical loading. The critical electric field and the critical mechanical load are functions of the crack size or the length of the electrode, while both the electrical fracture toughness and the mechanical fracture toughness are material properties. Thus, one can predict the critical electric field and the critical mechanical load when the sample geometry and the electrical fracture toughness and the mechanical fracture toughness are available.

The experimental results on electrically conductive cracks (deep notches) in poled lead zirconate titanate PZT-8 ceramics under mechanical and/or electrical loading verify the theoretical prediction of the CFZ model [18]. But, the experimentally determined coupling factor deviates from the theoretical predicted value [17]. This quantitative inconsistency prompts us to re-examine the CFZ model [19]. The concept of secant piezoelectric constant was introduced to refine the CFZ model and the refined CFZ model explained the experimental results perfectly [19]. The theoretical modification and the re-analysis of the experimental data indicate that the piezoelectric effect in the failure of conductive cracks in piezoelectric ceramics is reduced due to the high electric field at the crack tip [19]. The empirical fitting of the experimental results for both PZT-4 and PZT-8 ceramics under mechanical and/or electric (positive or negative) loading yields a coupling factor, which value is smaller than the corresponding value predicted from the CFZ model with the nominal piezoelectric constants. This strongly supports the rationale of using the secant piezoelectric constant. Although the absolute values of the experimental data exhibit great scattering and large difference between the PZT-4 and PZT-8 ceramics, the normalized experimental results can be predicted by the refined CFZ model. As described in the previous publications [16-19], the CFZ model is two-dimensional, in which electrical charges are treated as line charges per unit length and the line charges are allocated along a strip in front of a conductive crack tip. The two-dimensional CFZ model is able to capture the physical nature of the three-dimensional phenomena of electric charges emitted from a conductive crack tip and trapped in front of the tip. The distinctive advantage of the two-dimensional CFZ model lies in that it is simple and that the failure formula derived is easy to apply to engineering practices.

The purpose of the present study is to apply the CFZ model to interpret the experimental results obtained by Heyer *et al*. [13].

2. The Charge-Free Zone Model

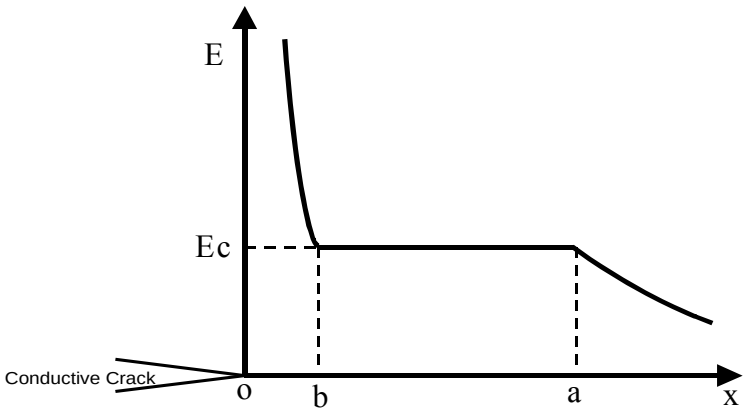

Fig. 2 The field distribution in front of a conductive crack, wherein *ob* is the size of the charge-free zone and *ba* the trapped charge zone.

The CFZ model is a two-dimensional model, in which charges are treated as line charges per unit length. Under applied electric loading, the high electric field at a conductive crack tip has the tendency to emit charges from the tip, while there are image forces acting on the charges, which are against the charge emission. Therefore, there must be a charge-free zone in front of the crack tip in order to emit charges continuously from the crack tip. These emitted charges are entrapped in the region of *ba*, as shown in Figure 2, where *ob* denotes the CFZ size. With the simplified constitutive equations, the CFZ model gives the local energy release rate [17]:

$$2G^{l} = \frac{1}{M}\left(K_{\sigma}^{a} - eK_{E}^{a}\right)^{2} + \kappa\left(\Omega K_{E}^{a}\right)^{2}, \tag{1}$$

where *M, e* and κ represent, on a qualitative basis, the elastic, piezoelectric and dielectric properties of the material, respectively, and

$$\Omega = \sqrt{\frac{b}{a}}\frac{F\left(\frac{\pi}{2}, \sqrt{1-\frac{b}{a}}\right)}{E\left(\frac{\pi}{2}, \sqrt{1-\frac{b}{a}}\right)}. \tag{2}$$

In Eq. (2), $F(\frac{\pi}{2},k)$ and $E(\frac{\pi}{2},k)$ are the complete elliptic integrals of the first kind and the second kind, respectively. The parameter Ω is defined as the ratio of the local electric intensity factor to the applied, i.e., $K_{E}^{l} = \Omega K_{E}^{a}$, which represents the shielding level of the trapped charges to the conductive crack tip. By using the local energy release rate as the failure criterion [17], the CFZ model leads to the following failure formula:

$$\left(\frac{K_{\sigma,C}^{a}}{K_{\sigma,C}^{o}}\right)^{2} \mp \frac{2e}{\left(e^{2}+\kappa M\Omega^{2}\right)^{1/2}}\left(\frac{K_{\sigma,C}^{a}}{K_{\sigma,C}^{o}}\right)\left(\frac{K_{E,C}^{a}}{K_{E,C}^{o}}\right) + \left(\frac{K_{E,C}^{a}}{K_{E,C}^{o}}\right)^{2} = 1, \tag{3}$$

where $K_{\sigma,C}^{o}$ (or $K_{E,C}^{o}$) is the mechanical (or electrical) fracture toughness under purely mechanical (or electrical) loading, $K_{\sigma,C}^{a}$ (or $K_{E,C}^{a}$) is the critical stress (or electric) intensity factor under combined mechanical and electrical loading. Note that the negative sign is for positive electric loading and positive sign is for negative electric loading. Mathematically, Eq. (3) has the form of $x^{2} + \eta xy + y^{2} = 1$ with $x = K_{\sigma,C}^{a} / K_{\sigma,C}^{o}$ (or $x = K_{E,C}^{a} / K_{E,C}^{o}$) and $y = K_{E,C}^{a} / K_{E,C}^{o}$ (or $y = K_{\sigma,C}^{a} / K_{\sigma,C}^{o}$), and $\eta = \mp 2e/\left(e^{2}+\kappa M\Omega^{2}\right)^{1/2}$, which is called the coupling factor. The mathematic equation can be expressed in the standard form of an ellipse, $\hat{x}^{2}/[2/(2+\eta)] + \hat{y}^{2}/[2/(2-\eta)] = 1$, where the $(\hat{x}, \hat{y})$ coordinator system is established by rotating 45° from the horizontal axis of the (x, y) coordinate system. The absolute value of η is less than two due to $\left(1+\kappa M\Omega^{2}/e^{2}\right)^{1/2} > 1$ and thus Eq. (3) indeed describes an ellipse in terms of the normalized applied intensity factors. In the case that the poling diction is along the positive *x*-direction, *e* is positive. Thus, if applied electric fields are parallel to the poling

direction, i.e., under positive electrical loading, $\eta < 0$ and the major semi-axis is located on the $\hat{x}$-axis, while $\eta > 0$ and the minor semi-axis is located on the $\hat{x}$-axis when applied electric fields are anti-parallel to the poling direction, i.e., under negative electrical loading. On the other hand, *e* is negative when the poling direction is along the negative *x*-direction. In this case, $\eta < 0$ and the major semi-axis is located on the $\hat{x}$-axis under negative electrical loading, i.e., when applied electric fields are parallel to the poling direction, whereas $\eta > 0$ and the minor semi-axis is located on the $\hat{x}$-axis under positive electrical loading, i.e., when applied electric fields are anti-parallel to the poling direction. For clarification and simplification, we may conclude that $\eta < 0$ and the major semi-axis is located on the $\hat{x}$-axis if applied electric fields are parallel to the poling direction and $\eta > 0$ and the minor semi-axis is located on the $\hat{x}$-axis if applied electric fields are anti-parallel to the poling direction. For dielectric materials, the piezoelectric constant, *e*, is zero and thus, the interaction term, i.e., the second term on the left hand-side of Eq. (3) disappears, thereby reducing Eq. (3) to the failure criterion for conductive cracks in dielectric materials [16].

3. Results and discussion

A great challenge in analysis of fracture and failure data of piezoelectric ceramics under mechanical and/or electrical loading is the large scattering of experimental data, which has been emphasized in previous publications [8, 20, 21]. That is why large number of tests has been repeated in the study of fracture and failure behaviors of conductive cracks [14-19]. Many repeated tests allow us to conduct a statistic analysis, which makes results more reliable.

In Heyer *et al.*'s experiment [13], the applied electric intensity factor changed from $30\,kV/m^{1/2}$ to $-90\,kV/m^{1/2}$. They did not measure the value of the electrical fracture toughness, $K^{o}_{E,C}$, under purely electrical loading. Therefore, we shall use Eq. (1) to analyze their data. Eq. (1) can be written as

$$2MG^{l} = \left(K^{a}_{\sigma} - eK^{a}_{E}\right)^{2} + M\kappa\Omega^{2}\left(K^{a}_{E}\right)^{2}. \tag{4}$$

Under purely mechanical mode I loading, the critical energy release rate is determined to be

$$2MG^{l}_{C} = \left(K^{o}_{\sigma,C}\right)^{2}. \tag{5}$$

Combining Eq. (5) and Eq. (4) yields

$$\left(K^{o}_{\sigma,C}\right)^{2} = \left(K^{a}_{\sigma,C} - eK^{a}_{E,C}\right)^{2} + M\kappa\Omega^{2}\left(K^{a}_{E,C}\right)^{2}. \tag{6}$$

Eq. (6) will be used to fit the experimental data [13] by using the least-squares method.

Figure 3 shows the fitting results, giving $\left(K_{\sigma,C}^{o}\right)^2$ =0.9167 $\left(MPa\sqrt{m}\right)^2$ or $K_{\sigma,C}^{o}$ =0.9574 $MPa\sqrt{m}$, $-2e=$ 12.3 C/m^2 or $e=$ -6.2 C/m^2, and $e^2+M\kappa\Omega^2=10.16$ (C/m^2)^2. The fitted value of the mechanical fracture toughness is almost the same as the measured one, as shown in Fig. 3. Actually, the measured data of mechanical fracture toughness of PZT ceramics scatters due to the brittle nature of the material. The fitting results show that the piezoelectric constant has a minus sign, which is consistent with the material properties listed in [13]. However, the fitted value of $e^2+M\kappa\Omega^2=10.16$ (C/m^2)^2 does not make sense to the CFZ model because the value of $e^2+M\kappa\Omega^2$ should be larger than or at least equal to e^2. If we assume the value of $M\kappa\Omega^2$ equal zero, Eq. (6) is reduced to

$$K_{\sigma,C}^{o}=K_{\sigma,C}^{a}-eK_{E,C}^{a}. \tag{7}$$

Eq. (7) shows the linear relationship between the applied mechanical stress intensity factor and the applied electric intensity factor. Applying Eq. (7) to fit the experimental data yields $e=$ -6.9 C/m^2 and $K_{\sigma,C}^{o}$ =0.9637 $MPa\sqrt{m}$, which are consistent with the fitting results with Eq. (6).

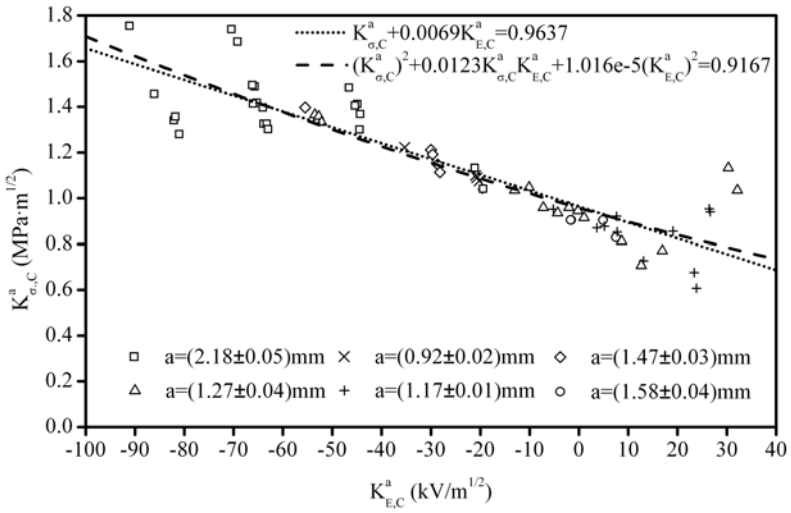

Fig. 3 Experimental data [13] and fitting curves with Eq. (6) and Eq. (7).

The inconsistence between the fitting results with Eq. (6) and the CFZ model might be caused by large data scattering and insufficient number of data. As indicated in Fig. 3, the two data at the applied electric intensity factors $K_{E,C}^{a}>30\,kV/m^{1/2}$ might be treated to be bad data. We eliminate the two bad data and fit the rest with Eq. (6) and Eq. (7) again, as plotted in Fig. 4. In this case, the linear fitting gives $K_{\sigma,C}^{o}$ =0.9368 $MPa\sqrt{m}$ and $e=$ -7.5 C/m^2. The nonlinear

fitting leads to $K^{o}_{\sigma,C}$ =0.9409 $MPa\sqrt{m}$, e = -8.6 C/m^2, and $e^2 + M\kappa\Omega^2 = 100$ (C/m^2)^2, thereby resulting in $M\kappa\Omega^2 = 26.04$ (C/m^2)^2. The Young's modulus, M, and the dielectric constant, κ, are at the orders of 10^{11} Pa and $10^3\kappa_0 \approx 10^{-8}$ C/(Vm), respectively, where $\kappa_0 = 8.85\times10^{-12}$ C/(Vm) is the dielectric constant of vacuum. As described above, the parameter Ω is defined as the ratio of the local electric intensity factor to the applied, representing the shielding level of the trapped charges to the conductive crack tip and its mathematical expression is given by Eq. (2). From the fitting result of $M\kappa\Omega^2 = 26.04$ (C/m^2)^2, we may estimate the parameter Ω to be 0.16, which is smaller than the values obtained for PZT-4 and PZT-8 ceramics [19]. The small value of the parameter Ω implies that the applied electric field is greatly shielded by the charge zone. This case might occur if the charge-free zone is extremely small, as indicated by Eq. (2).

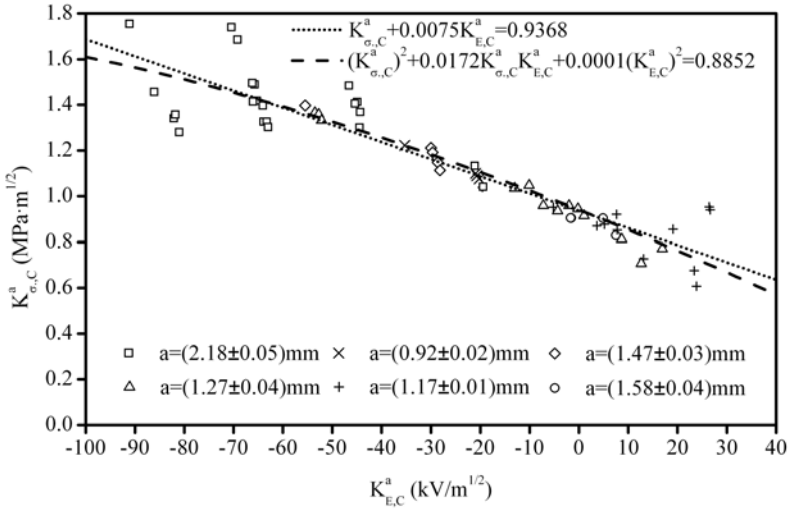

Fig. 4 Experimental data except of two bad data at the applied electric intensity factors $K^a_{E,C} > 30\,kV/m^{1/2}$ [13] and fitting curves with Eq. (6) and Eq. (7).

4. Concluding remarks:

The present work demonstrates that the CFZ model can be successfully applied to interpret the experimental results on poled lead zirconate titanate PIC 151 ceramics. Although there is large data scattering, the CFZ model can fit them with a wider range in comparison with the fitting based on the domain switching model [13]. The fitted material properties are at the same order as these listed in Reference [13], which indicates that if we conduct a numerical analysis based on Stroh formalism with the material properties, we should be able to predict the fracture behavior, which will be done soon. The advantage of the simplified constitutive equations lies in that the failure criterion given by Eq. (1) is simple

and user-friendly. However, there is a parameter Ω that has to be determined from fitting experimental results at the moment.

Acknowledgements:

This work was supported by a RGC grant from the Hong Kong Research Grants Council, HKSAR, China. The author thanks Mr. Zhijia Wang for his help in plotting the figures.

References:

[1] B.L. Wang, Y.W. Mai, An electrode analysis for multilayer ceramic actuators, Sensors & Actuators A - Physical 121 (2005) 203-212.
[2] Z. Suo, Models for breakdown-resistant dielectric and ferroelectric ceramics, J Mech Phys Solids 41 (1993) 1155-1176.
[3] T.Y. Zhang, P. Tong, Fracture mechanics for a mode III crack in a piezoelectric material. Int J Solids Struct 33 (1996) 343-359.
[4] H. Gao, T.Y. Zhang, P. Tong, Local and global energy release rates for an electrically yield crack in piezoelectric ceramics, J Mech Phys Solids 45 (1997) 491-510.
[5] T.Y. Zhang, C.F. Qian, P. Tong, Linear electro-elastic analysis of a cavity or a crack in a piezoelectric material, Int J Solids Struct 35 (1998) 2121-2149.
[6] R.M. McMeeking, Towards a fracture mechanics for brittle piezoelectric and dieletric materials, Int J Fract 108 (2001) 25–41.
[7] W. Yang, Mechatronic Reliability, Tsinghua University Press and Springer, Beijing, 2001.
[8] T.Y. Zhang, M.H. Zhao, P. Tong, Fracture of piezoelectric ceramics, Advances in Appl Mech 38 (2002) 147-279.
[9] Y.H. Chen, T.J. Lu, Cracks and fracture in piezoelectrics, Advances in Appl Mech 29 (2003) 121-215.
[10] T.Y. Zhang, C.F. Gao, Fracture behaviors of piezoelectric materials, Theor Appl Fract Mech 41 (2004) 339-379.
[11] G.A. Schneider, Influence of electric field and mechanical stresses on the fracture of ferroelectrics, Annu Rev Mater Res 37 (2007) 491-538.
[12] E.J. Garboczi, Linear dielectric breakdown electrostatics, Phys Rev B 38 (1988) 9005-9010.
[13] V. Heyer, G.A. Schneider, H. Balker, J. Drescher, H.A. Bahr, A fracture criterion for conducting cracks in homogeneously poled piezoelectric PZT-PIC 151 ceramics, Acta Mater 46 (1998) 6615-6622.
[14] T. Wang, T.Y. Zhang, Electrical fracture toughness for electrically conductive deep notches driven by electric fields in depoled lead zirconate titanate ceramics, Appl Phys Lett 79 (2001) 4198-4200.

[15] R. Fu, C.F. Qian, T.Y. Zhang, Electrical fracture toughness for conductive cracks driven by electric fields in piezoelectric materials, Appl Phys Lett 76 (2000) 126-128.
[16] T.Y. Zhang, T. Wang, M.H. Zhao, Failure behavior and failure criterion of conductive cracks (deep notches) in thermally depoled PZT-4 ceramics, Acta Mater 51 (2003) 4881-4895.
[17] T.Y. Zhang, M.H. Zhao, G. Liu, Failure behavior and failure criterion of conductive cracks (deep notches) in piezoelectric ceramics I – the charge-free zone model, Acta Mater 52 (2004) 2013–2024.
[18] T.Y. Zhang, G. Liu, Y. Wang, Failure behavior and failure criterion of conductive cracks (deep notches) in piezoelectric ceramics II: experimental verification, Acta Mater 52 (2004) 2025–2035.
[19] T.Y. Zhang, G. Liu, T. Wang, P. Tong, Application of the concepts of fracture mechanics to the failure of conductive cracks in piezoelectric ceramics, Eng Fract Mech 74 (2007) 1160-1173.
[20] R. Fu, T.Y. Zhang, Effect of an applied electric field on the fracture toughness of lead zirconate titanate ceramics, J Am Ceram Soc 83 (2000) 1215-1218.
[21] R. Fu, T.Y. Zhang, Influence of temperature and electric field on the bending strength of lead zirconate titanate ceramics, Acta Mater 48 (2000) 1729-1740.